*Manuscript with continous line numbering
Click here to view linked References

Effects of warming on the degradation and production of low-molecular-weight labile organic carbon in an Arctic tundra soil

Ziming Yang[1], Stan D. Wullschleger[1,2], Liyuan Liang[1], David E. Graham[2,3], Baohua Gu[1*]

[1] Environmental Sciences Division, Oak Ridge National Laboratory, Oak Ridge, Tennessee, United States of America

[2] Climate Change Science Institute, Oak Ridge National Laboratory, Oak Ridge, Tennessee, United States of America

[3] Biosciences Division, Oak Ridge National Laboratory, Oak Ridge, Tennessee, United States of America

***** Corresponding author: Phone: (865)-574-7286; Email: gub1@ornl.gov

Disclaimer:

This manuscript has been authored by UT-Battelle, LLC under Contract No. *DE-AC05-00OR22725* with the US Department of Energy (DOE). The United States Government retains and the publisher, by accepting the article for publication, acknowledges that the United States Government retains a non-exclusive, paid-up, irrevocable, world-wide license to publish or reproduce the published form of this manuscript, or allow others to do so, for United States Government purposes. The Department of Energy will provide public access to these results of federally sponsored research in accordance with the DOE Public Access Plan (http://energy.gov/downloads/doe-public-access-plan).

Abstract

The fate of soil organic carbon (SOC) stored in the Arctic permafrost is a key concern as temperatures continue to rise in the northern hemisphere. Studies and conceptual models suggest that degradation of SOC is affected by its composition, but it is unclear exactly which SOC fractions are vulnerable to rapid breakdown and what mechanisms may be controlling SOC degradation upon permafrost thaw. Here, we examine the dynamic consumption and production of labile SOC in an anoxic incubation experiment using soil samples from the active layer at the Barrow Environmental Observatory, Barrow, Alaska, USA. Free-reducing sugars, alcohols, and low-molecular-weight (LMW) organic acids were analyzed during incubation at either –2 or 8 °C for up to 240 days. Results show that degradation of simple sugar and alcohol in SOC largely accounts for the initial rapid release of CO_2 and CH_4 through anaerobic fermentation, whereas the fermentation products, acetate and formate, are subsequently utilized as primary substrates for methanogenesis. Iron(III) reduction is correlated with acetate production and methanogenesis, suggesting its important role as an electron acceptor in SOC respiration in tundra environment. These observations are further supported in a glucose addition experiment, in which rapid CO_2 and CH_4 production occurred concurrently with rapid production and consumption of labile organics such as acetate. However, addition of tannic acid, as a more complex organic substrate, showed little influence on the overall production of CO_2 and CH_4 and organic acids. Together our study shows that LMW labile SOC controls the initial rapid release of green-house gases upon warming of permafrost soils. We present a conceptual framework for the labile SOC transformations and their relations to fermentation, iron reduction and methanogenesis, thereby providing the basis for improved model prediction of climate feedbacks in the Arctic.

Keywords: soil carbon degradation, climate warming, anaerobic fermentation, methanogenesis, biogeochemistry, Arctic tundra

1. Introduction

Arctic soils represent a large organic carbon pool, and it is estimated that approximately half of terrestrial soil organic carbon is associated with permafrost in high-latitude ecosystems (Schuur et al., 2008; Tarnocai et al., 2009; Hugelius et al., 2014). Climate warming is expected to increase permafrost thaw, both in depth and duration, that could trigger substantially increased degradation of frozen soil organic matter and the release of CH_4 and CO_2 to the atmosphere (Schuur et al., 2009; 2015; McCalley et al., 2014; Koven et al., 2015; Tveit et al., 2015). The effect of thawing permafrost is inevitably associated with increased microbial activity and SOC decomposition (Lipson et al., 2012; Lipson et al., 2013), yet it remains largely unknown what and how fast SOC degrades in water-saturated tundra soil under warming. Numerous field and laboratory short-term studies have observed an initial rapid release of CO_2 and CH_4 upon warming, followed by declines in carbon loss rates over time (Waldrop et al., 2010; Lee et al., 2012; Roy Chowdhury et al., 2015; Treat et al., 2015; Schuur et al., 2015), as more labile carbon pools are preferentially degraded (Drake et al. 2015). Conceptual models suggested that this initial, rapid degradation is related to, among other factors, the potential of SOC to decompose (i.e., decomposability) (Schuur et al., 2015), but it is not clear at the molecular level what specific types of SOC are susceptible to rapid breakdown upon thaw. This lack of mechanistic understanding of the biogeochemistry of SOC limits our ability to build process-based models in predicting carbon cycling and future climate change in the Arctic (Riley et al., 2011; Graham et al., 2012; Tang and Riley, 2015). It highlights the need for long-term detailed studies of SOC compositional changes, particularly the production and consumption of labile SOC in relation to CH_4 and CO_2 dynamics (Treat et al., 2015) and the degradation rates of permafrost-associated SOC.

We hypothesized that SOC degradation rates are correlated to its composition, i.e., certain types of SOC are more labile and susceptible to rapid breakdown than the other C pools

(Hernández and Hobbie, 2010; Pare and Bedard-Haughn, 2013; Jagadamma et al., 2014; Wild et al., 2014; Drake et al. 2015), resulting in initial rapid release of CO_2 and CH_4 upon warming. To test this hypothesis, we monitored the production and consumption of low-molecular-weight (LMW) labile organic compounds such as reducing sugars, ethanol, and acetate during anaerobic incubations with both active-layer organic and mineral soils from a continuous permafrost field site on the Coastal Plain of Alaska. Additionally, we separately studied degradation of glucose, as a simple carbohydrate, and tannic acid, as a more complex polyphenolic compound, during the incubation. Based on previous studies (Lipson et al., 2010; Lipson et al., 2013), we also examined the role of ferric ion, serving as an important electron acceptor, in SOC respiration and methanogenesis. Using a suite of analytical techniques, we characterized specific labile organic compounds, including C_1-C_4 organic acids, alcohols, and reducing sugars, in the organic and mineral soil layers during incubations at either –2 or 8 °C to mimic the near-freezing and maximum thaw conditions at the Barrow field site in Alaska, USA (Roy Chowdhury et al., 2015). Our study specifically addresses the effect of thaw on transformations of labile SOC and the dynamic changes in C flow through fermentation intermediates to CH_4 and CO_2 emissions.

2. Materials and methods

2.1. Soil sampling and processing

Frozen soil cores were collected in April 2012 (average temperature, –15 ºC) from trough areas of a high-center polygon (N 71º16.757' W 156 º36.274) at the Barrow Environmental Observatory (BEO) in northern Alaska, as described previously (Roy Chowdhury et al., 2015). A coring auger (manufactured by Jon's Machine Shop in Fairbanks, AK) mounted on a sled was used to collect ~1 m length soil cores in clear PVC liners (3" diameter × 36" length) that were sterilized with ethanol prior to use. Soil cores were kept frozen during shipment and stored at –20 ºC till the day of processing inside an anoxic glove chamber under a N_2 atmosphere (Coy, Grass

Lake, MI). Soil cores were placed on frozen blue ice packs to minimize thaw and a power oscillating tool with sterilized cutting blades was used to section, then homogenize the soil cores in autoclaved containers. Different soil layers were identified by both moist soil Munsell color and the soil chemistry analysis (Table S1). The organic-rich (8-20 cm below ground surface) and the mineral-rich (22-45 cm below surface) soils in the active layer were separated for the incubation study. The very top of the organic layer consisting plant materials and the bottom ice wedge layer were excluded from the incubation.

2.2. Soil microcosm incubations

The thawed and homogenized wet soil subsamples (150 ± 0.5 g) were then transferred into autoclaved and N_2-purged glass bottles (600 mL, VWR International) in the anoxic chamber. They were subsequently sealed tightly with thick butyl rubber stoppers and capped. Soil samples were subsequently taken and analyzed at selected time intervals from once a week for the first two months of incubation and then once every two weeks after 60 days. The headspace was evacuated (with a vacuum pump) and flushed at least three times with N_2 after each sampling event to remove residual CO_2 and CH_4 for subsequent measurements of the CO_2 and CH_4 production. Net CO_2 and CH_4 production was calculated by subtracting any remaining CO_2 and CH_4 in solution after N_2 purging. All samples were incubated in the dark at two temperatures (–2 ^oC and 8 ^oC). Three replicates per temperature per soil layer in separate bottles were incubated for up to 240 days under anoxic conditions.

At the later stage of the microcosm experiments, glucose and tannic acid were added to soil incubations at 8 °C to study their effects on SOC anaerobic respiration and transformations. Dissolved D-(+)-glucose (Sigma Aldrich) in water (0.1 M) was added at day 144 when the degradation or production of CO_2 and CH_4 reached a steady state. Only a small volume (<1 mL) was introduced to the soil, well mixed using a spatula, to minimize effects on the soil water

content and soil chemistry. The total amounts of glucose added to the organic and mineral soils were 6.0 ± 1.0 and 0.5 ± 0.1 μmol of glucose-C g^{-1} dwt. soil (dry weight of soil), respectively, comparable to the amounts of reducing sugars in the initial soil. The reducing sugar concentrations were then monitored periodically, along with CO_2 and CH_4 production, organic acids, alcohols, and Fe concentrations, as described above. Tannic acids (JT Baker) were then added on day 188 after observing that the production of CO_2 and CH_4 (or organic acids) reached a new steady state. Similar to the glucose addition on day 144, only a small amount of tannic acid was added, equivalent to 5 and 0.5 μmol of tannic acid g^{-1} dwt. soil to the organic and mineral layer soils, respectively.

2.3. Analytical techniques

Headspace CO_2 and CH_4 were analyzed with a gas chromatograph (GC) equipped with a methanizer and a flame ionization detector (SRI 8610C, SRI Instruments, Torrance, CA) with He as the carrier gas. A gas-tight syringe was used first to mix the gas by drawing and pumping the headspace gas several times in each sealed incubation bottle, and then to take a 0.5 mL of headspace gas sample and immediately injected into the GC for analysis. Calibration with gas standards (99.99%; Scotty Specialty Gas Calibration Standards, Sigma Aldrich) was performed prior to the sample analysis. Gas production rates (μmol g^{-1} dwt. soil day^{-1}) were estimated by the change of gas concentrations between every two adjacent measured time points during incubation. The dissolved gas concentrations were calculated using Henry's law after correcting for temperature and soil pH. Subsamples (n=3) of the organic and mineral soils were taken for the determination of water content, soil pH, total C and N using similar methods as described previously (Roy Chowdhury et al., 2015).

Aliquots of wet soil samples (1–2 g from the 600-mL incubation) were taken at pre-determined time intervals and subsequently equilibrated with either 10 mM NH_4HCO_3 (pH ~ 7.3)

149 or 0.1 M KCl (pH ~ 5.0) solution. The NH_4HCO_3 extraction (6 h) was used for determining
150 soluble soil organic matter compositions, whereas the KCl extraction (2 h) was used to determine
151 exchangeable and dissolved inorganic species including Fe(II), Fe(III), major anions and cations.
152 Samples were centrifuged for 15 min at 6,500 × *g*, and the supernatants were collected and
153 subsequently filtered through 0.45-μm membrane filters before analysis. Exchangeable Fe(II)
154 concentrations from filtered KCl extract samples were quantified using the HACH (Loveland,
155 Colorado) Ferrous method 8146 (1,10-phenanthroline) on a HACH DR 900 colorimeter, whereas
156 the total dissolved iron concentrations were determined using the HACH FerroVer method 8008.
157 Samples were diluted as necessary, and the colorimeter was calibrated with standards in the
158 concentration range of 0.02 to 3.0 mg/L prior to the analysis.

159 Total dissolved organic carbon (DOC) was measured by combustion on a Shimazdu
160 TOC-L analyzer (Shimazdu Corp.), where the extract samples and analytical blanks were first
161 acidified with 6 N HCl and purged sufficiently to remove any dissolved inorganic carbonates.
162 Organic acids (formate, acetate, propionate, butyrate, succinate, fumarate, and citrate) and
163 inorganic anions (chloride, sulfate, nitrate, and phosphate) were measured by a Dionex DX500
164 ion chromatograph (IC) equipped with a Dionex IonPac AS15-5μm analytical column and an
165 AG15 guard column. Calibration curves for each analyte were established using the standard
166 compounds. Alcohols (methanol, ethanol, 2-propanol and 1-butanol) were measured using a GC
167 equipped with a flame ionization detector (Agilent Technologies) and a Stabilwax polyethylene
168 glycol column (30m × 0.53mm × 1.00μm; Restek, Bellefonte, PA). Simple sugars (e.g., glucose)
169 were measured with a refraction index detector on a Breeze 2 high-performance liquid
170 chromatography (HPLC) system (Waters, Milford, MA) using an Aminex HPX-87H column
171 (Bio-Rad Laboratories, Hercules, CA).

172 Concentrations of reducing sugars in extracted mono- and polysaccharides were
173 determined using previously established methods (Myklestad et al., 1997; Hung et al., 2001). In

brief, the extract samples were diluted with 1N HCl and added to 10-mL glass ampules (Wheaton), which were then sealed and placed in an oven at 120 ºC for 3 hrs. After complete hydrolysis, 1N NaOH was added into the ampules to neutralize the sample, which was subsequently mixed with 0.7 mM potassium ferricyanide and placed in the boiling water bath for 10 min in the dark. Then, 2 mM ferric chloride and 2.5 mM 2,4,6-tripyridyl-s-triazine (TPTZ, SigmaAldrich) in 3 M acetic acid were added immediately and well-mixed. The absorbance of the ferrous-TPTZ complexes was measured at 596 nm using an ultraviolet-visible (UV-Vis) spectrophotometer (Hewlett-Packard 8453). Since Fe(II) in the diluted extract samples interferes with the TPTZ absorbance, its concentration was corrected by using results from parallel reactions at 25 ºC (instead of 120 ºC) under which condition hydrolysis of the carbohydrates was minimized. The corrected concentrations of free-reducing sugars were reported as μmol glucose-C g^{-1} dwt. soil.

2.4. Statistical analysis

Correlations between CH_4/CO_2 ratios, Fe(II)/Fe(tot) ratios, and acetate concentrations were analyzed using linear regression in Origin v8.6 (OriginLab Corporation, Northampton, MA), and differences were analyzed using one-way ANOVA. Effects of incubation time and soil types (organic and mineral) on CH_4 and CO_2 production rates, cumulative concentrations of reducing sugars, ethanol, and organic acids were also evaluated using ANOVA. The tests were computed using the R statistical package (v3.0.3) (R Core Team, 2013).

3. Results

3.1. CO_2 and CH_4 production

3.1.1. Temperature sensitivity

Incubation over the first 144 days at 8 ºC produced CO_2 and CH_4 at 90 ± 9 and 14 ± 1 μmol g^{-1} dwt. soil in the organic layer and 23 ± 2 and 13 ± 1 μmol g^{-1} dwt. soil in the mineral layer, representing a total degradation of SOC of 104 ± 10 and 36 ± 3 μmol g^{-1} dwt. of the organic and mineral soils, respectively (Fig. S1). The calculated CO_2 and CH_4 production rates varied with both soil layers and the incubation time (Fig. 1). The CO_2 production rate was approximately an order of magnitude higher in the organic layer than in the mineral layer (P < 0.001). The highest rate was observed initially (3.0 μmol g^{-1} soil day^{-1} in the organic layer and 0.3 μmol g^{-1} soil day^{-1} in the mineral layer) and then decreased gradually until day 144, the trend similar to those reported previously (Roy Chowdhury et al. 2014). The production rate of CH_4 was significantly lower than CO_2, but was comparable between the organic and the mineral layer (Fig. 1). The ratio of CH_4/CO_2 production rates in the organic layer increased progressively with the incubation time and, in the mineral layer, it rapidly approached 0.65 at day 30 and then stabilized (Fig. 2). The observed ratios of CH_4/CO_2 in the mineral layer were also significantly higher than that in the organic layer throughout the incubation (P < 0.001).

Substantially lower amounts of organic C were degraded in both the organic (30 ± 5 μmol C g^{-1}) and the mineral (6 ± 1 μmol C g^{-1}) soils at –2 ºC than at 8 ºC. For the organic layer, the initial rates of CO_2 and CH_4 were only 0.2 and 0.001 μmol g^{-1} dwt. soil day^{-1}, compared to 3.0 and 0.1 μmol g^{-1} dwt. soil day^{-1} of CO_2 and CH_4 production at 8 ºC, respectively. For the mineral layer, the production rates were also an order of magnitude lower than those at 8 ºC (P < 0.001). In contrast to the general decreasing trend at 8 ºC, increasing rates of CO_2 and CH_4 production were observed after 20 days in both organic and mineral layers (Fig. 1c, d). In addition, the rate

ratio of CH_4/CO_2 production also increased significantly with time in both soil layers (Fig. 2c, d) ($P < 0.01$). However, the CH_4 production rate and CH_4/CO_2 rate ratios in the organic layer were substantially lower than that in the mineral layer ($P < 0.001$).

3.1.2. Incubation with glucose and tannin addition

Prior to the glucose addition on day 144, the production rates of CO_2 and CH_4 at 8 ºC maintained steadily at ~ 0.2 and 0.06 μmol g^{-1} dwt. soil day^{-1} for the organic layer, and ~ 0.15 and 0.1 μmol g^{-1} dwt. soil day^{-1} for the mineral layer, respectively. After the glucose addition (6 ± 1.0 μmol C g^{-1} dwt. organic soil and 0.5 ± 0.1 μmol C g^{-1} dwt. mineral soil), CO_2 and CH_4 production rapidly increased in both the organic and mineral layer soils (Fig. 1). For organic layer, the highest production rates were 1.0 μmol g^{-1} dwt. soil day^{-1} for CO_2 and 0.2 μmol g^{-1} dwt. soil day^{-1} for CH_4, which are about 5 and 3 times of those before the glucose addition. Similarly in the mineral layer, the maximum CO_2 and CH_4 production rates increased to 0.4 and 0.3 μmol g^{-1} dwt. soil day^{-1}, representing an enhancement factor of 3. Addition of glucose also had a significant impact on the CH_4/CO_2 production ratio, which exhibited a dramatic decrease within the first few days, and then increased rapidly to the previous level of 0.3 on day 188 (Fig. 2a) ($P < 0.01$). The CH_4/CO_2 ratios in the mineral layer showed a similar "decrease and increase" pattern (Fig. 2b), but the changes were smaller than those observed in the organic layer.

Addition of tannic acid, a complex polyphenolic, lignin-type organic compound, did not appreciably enhance the production of CO_2 and CH_4 in both soil layers at 8 ºC. Although similar amounts of substrate C (5 and 0.5 μmols g^{-1} dwt. soil in organic and mineral layer, respectively) were added on day 188, the production of CO_2 and CH_4 only slightly increased in the organic layer but decreased in the mineral layer (Fig. 1) ($P < 0.02$). A small decrease in CH_4/CO_2 ratio was also observed in both organic and mineral layers (Fig. 2) ($P < 0.01$) as a result of tannin addition.

3.2. Consumption and production of reducing sugars, alcohols, and organic acids

During the 240 day of incubation, the total dissolved organic carbon (DOC) in the NH_4HCO_3 extract was nearly constant, at 400 ± 20 and 50 ± 8 μmol C g^{-1} dwt. soil in the organic and mineral layer, respectively. Bulk analysis of total organic C (22.5 mmol C g^{-1} dwt. soil in the organic layer and 11.6 mmol C g^{-1} dwt. soil in the mineral layer) also showed no significant changes in SOC content during the entire incubation, because the cumulative production of CO_2 and CH_4 represented < 1% of total SOC. To understand the mechanisms and pathways of SOC degradation, detailed analyses of composition changes in SOC were performed during incubation to determine the types of organics that are more susceptible to breakdown.

3.2.1. Reducing sugars and alcohols

Results indicate that free-reducing sugars were quickly consumed from 15 to 9 ± 1 μmol glucose-C g^{-1} dwt. soil in the first 20 days in the organic layer at 8 ºC (Fig. 3a), leading to the initial rapid production of CO_2, CH_4, ethanol, and acetate (details below). The consumption of reducing sugars also occurred at lower temperature (–2 ºC), albeit at a slow rate of ~0.12 μmol g^{-1} dwt. soil day^{-1} in the first 50 days. Similarly in the mineral layer, rapid depletion of reducing sugars occurred at 8 ºC (Fig. 3b), despite of a low initial concentration of reducing sugars (1 μmol glucose-C g^{-1} dwt. soil, or about 15 times lower than that in the organic layer). Concurrent production and consumption of primary alcohols were also observed in the system (Fig. 3c, d), where an initial increase of ethanol concentration in both organic and mineral layers corresponded well with rapid degradation of reducing sugars in the first 20 days of incubation. Methanol, 2-propanol, and 1-butanol were also detected but not shown due to their substantially lower concentrations than ethanol. Over time, however, ethanol was consumed, and its concentration decreased from about 9 to 2 μmol g^{-1} dwt. soil between day 20 and 120 in the organic layer, and from about 3 to 0.5 μmol g^{-1} dwt. soil in the mineral layer ($P < 0.001$).

Consistent patterns were observed following glucose addition at day 144. There was a rapid increase of CO_2 and CH_4 gas production (Fig. 1a, b) as well as ethanol production a few days after glucose addition (Fig. 3c, d). Ethanol was then quickly consumed resulting in the production of simple organic acids such as acetate and propionate (described below). In comparison, addition of tannic acid at day 188 did not increase the ethanol concentration.

3.2.2. Organic acids

We observed a distinct pattern of dynamic changes in LMW organic acids including formate, acetate, propionate, and butyrate (Fig. 4). Acetate, propionate, and butyrate all accumulated with incubation time at 8 ºC in the organic layer (Fig. 4a), except that formate was below the detection limit (<1 μM) after 60 days. Prior to the glucose addition, the concentration of acetate increased progressively from 18 to 35 ± 3 μmol g^{-1} dwt. soil and the propionate concentration increased from 0 to 10 ± 2 μmol g^{-1} dwt. soil, while the butyrate concentration increased rapidly in the first 20 days to 15 ± 3 μmol g^{-1} dwt. soil and thereafter stabilized at a similar value. However, in contrast to those observed in the organic layer, the organic acid production in the mineral layer at 8 ºC was much lower ($P < 0.001$) (Fig. 4b), and they were mostly consumed within two months. Formate and acetate were consumed in 30 days, whereas propionate slightly accumulated within the first 20 days but subsequently decreased and consumed in ~2 months. The overall acid concentrations were lower than 0.2 μmol g^{-1} dwt. soil after day 70. Butyrate, which was accumulated at relatively high levels in the organic layer, was not observed in the mineral soil.

At –2 ºC, however, the accumulation of acetate was not observed in the organic layer (Fig. 4c). Instead, acetate was consumed from about 19 to 5 μmol g^{-1} dwt. soil between day 30 and 60 and, interestingly, butyrate increased from 3 to 11 μmol g^{-1} dwt. soil during the same time. Formate and propionate concentrations remained below 1 μmol g^{-1} dwt. soil throughout the entire

290 incubation (Fig. 4c). For the mineral layer, both acetate and propionate showed an overall
291 slightly increasing trend (Fig. 4d), compared to the decreasing trend at 8 ºC.

292 The patterns of the consumption of reducing sugars, the production followed by
293 consumption of ethanol, and changes in organic acids are also clearly illustrated following the
294 glucose addition. The added glucose was depleted within just a few days, leading to rapid
295 accumulation of fermentation products (i.e., ethanol and acetate) and increased CO_2 and CH_4 gas
296 production. A notably increased acetate concentration (~ 8 μmol g^{-1} dwt. soil) was detected
297 within 3 days after glucose addition in the organic layer ($P < 0.001$) (Fig. 4a). Slightly increased
298 production of butyrate and propionate accompanied with the acetate production ($P < 0.04$).
299 Concurrent with the acetate increase, ethanol concentration increased to 2 μmol g^{-1} dwt. soil on
300 day 150 (Fig. 4a). The integrated production of CO_2 and CH_4 from day 144 to 150 was 3.5 and
301 1.5 μmol g^{-1} dwt. soil (Fig. 1a), respectively, representing a carbon mass balance of 90 ± 10 % by
302 including both the consumption and production of various C substrates (i.e., organic acids,
303 alcohols, and gases) in the calculation. In particular, we observed a sharp decrease in CH_4:CO_2
304 ratio on day 150 ($P < 0.001$) following the glucose addition (Fig. 2a), indicating rapidly increased
305 CO_2 production relative to CH_4 production.

306 Addition of glucose also stimulated the ethanol and organic acid production in the
307 mineral layer. About 0.5 μmol ethanol g^{-1} dwt. soil was produced within the first few days after
308 glucose addition (Fig. 3d), which coincided with the consumption of 0.5 μmol glucose g^{-1} dwt.
309 soil (Fig. 3b). The highest concentrations of acetate and propionate were 0.2 and 0.15 μmol g^{-1}
310 dwt. soil, respectively (Fig. 4d). The cumulative production of CO_2 and CH_4 between day 144
311 and 150 were 2 and 1.8 μmol g^{-1} dwt. soil, respectively (Fig. 1), representing an estimated C mass
312 balance of 94 ± 8 %.

313

4. Discussion

The present study demonstrates that LMW labile SOC in Arctic soils plays an important role in controlling the initial rapid degradation of SOC and CH_4 and CO_2 emissions upon thaw. The peak production of CH_4 and CO_2 is well correlated to the concentration changes of easily-degradable SOC, including reducing sugars, alcohol, and acetate at the beginning of the incubation. This observation is further supported by glucose addition at the later stage of the incubation experiment, in which a spike in the production of CO_2 and CH_4 corresponded to rapid consumption of glucose, followed by the production and consumption of ethanol and acetate. In contrast, addition of a more complex organic substrate, tannin, showed little change in the production of CO_2 and CH_4. Neither did it influence the production or consumption of ethanol and organic acids. As a polyaromatic compound, tannin is too oxidized to ferment to ethanol but may potentially inhibit certain anaerobic microorganisms (Tavendale et al., 2005). The results from analyses of labile SOC during incubation and from the glucose and tannin addition experiments collectively suggest that organic substrate composition is an important factor affecting SOC degradation rates. Consistent with previous studies, soil organic matter with high contents of labile SOC is decomposed more rapidly than that with relatively high recalcitrant SOC (Fierer et al., 2005; Grogan and Jonasson, 2005; Hernández and Hobbie, 2010; Pare and Bedard-Haughn, 2013). The input and production of easily degradable SOC can stimulate the microbial activities that facilitate rapid SOC mineralization, and consequently CO_2 and CH_4 emission in Arctic soils (Waldrop et al., 2010; Wild et al., 2014; Drake et al. 2015). Our observed dynamic changes in simple organic acids, alcohols, and reducing sugars in both organic and mineral soils, reflect a net balance between the production and degradation of these organic substrates. We found that ~50% of the DOC turned over to CO_2 or CH_4 during the experiment, and that the composition of the DOC changed over time, but the bulk soil organic C and the total organic carbon did not change appreciably during the entire incubation. Thus the DOC

339 composition is highly dynamic with SOC degradation that produces DOC balanced by
340 mineralization and methanogenesis. Based on these findings, we propose the following scheme
341 of SOC degradation pathways in the active layer upon permafrost thaw: (1) increasing
342 temperature facilitates anaerobic fermentation to break down simple carbohydrates such as
343 reducing sugars to form ethanol and organic acids; (2) the ethanol is oxidized to form acetate; and
344 (3) acetate accumulates and decomposes through iron reduction or methanogenesis to form CH_4
345 or CO_2, or (4) acetate converts to butyrate (Fig. 5), consistent with our recent field observations
346 (Herndon et al., 2015).

347 As described earlier, rapid decomposition of free reducing sugars is closely associated
348 with rapid accumulation of ethanol and acetate during early incubation and in the glucose
349 addition experiments (Fig. 3, 4). Recent metagenomics studies showed that genes encoding
350 ethanol-producing enzymes can make up 27% of all fermentation genes in Arctic ocean
351 sediments (Kirchman et al., 2014). As an intermediate, ethanol is known to undergo anaerobic
352 oxidation in soils (Schink et al., 1985; Metje and Frenzel, 2005), including its partial oxidation to
353 acetate in anoxic peatland soil microcosms (Horn et al., 2003). Acetate can be further converted
354 into butyrate which accumulates in soils (Metje and Frenzel, 2005). In our microcosms, a
355 decreased ethanol concentration occurred with concomitant increase of acetate concentration
356 (Fig. 3, 4). Acetate generally undergoes acetoclastic methanogenesis to produce CH_4 and CO_2
357 (Lovley and Phillips, 1986; Schulz and Conrad, 1996; Hines et al., 2008; Hershey et al., 2014),
358 and this is evidenced by the consumption of acetate with simultaneous increase of CH_4 and CO_2
359 in the mineral soils (Fig. 4b). In the organic layer, however, acetate steadily increased with
360 incubation time (Fig. 4a), suggesting that the production of acetate through fermentation is
361 greater than the consumption by methanogenesis, because of the abundance of SOC in the
362 organic layer, as observed previously in northern wetlands (Hines et al., 2001; Duddleston et al.,
363 2002). Acetate concentration differences in the organic and mineral layers also suggest that the

accumulated acetate in the organic layer could be transported into the deeper and more anaerobic mineral layer to support Fe(III) reduction and methanogenesis. Transport of these organics through vertical movement of DOC or mixing through cryoturbation between the organic and mineral layer soils has been documented (Drake et al. 2015) and is evident since notable amounts of the organic substrates are found in the initial mineral soil (Figs. 3 and 4).

The present study focuses on the high-center polygon trough soils, which are saturated and anoxic at field conditions. The microbial processes we document here are different from other oxic soil horizons that occur across polygonal landscapes or from aerobic incubations which can result in an extremely high degradation rate of labile SOC (i.e., acetate and butyrate at 20°C) (Drake et al. 2015). Anaerobic fermentation is one of the primary processes that occur at the early stage of permafrost thaw, where it provides energy and simple organic substrates such as ethanol and acetate for subsequent methanogenesis and Fe(III) reduction. Fermentation and methanogenesis activities were observed in the present study, as indicated by the increase of CO_2 and CH_4/CO_2 ratio in both organic and mineral layers (Figs. 1 and 2). Importantly we observe that production and consumption of the organic acids coincided with the CH_4:CO_2 production ratios. For instance, in the organic layer at 8°C, acetate concentration is positively correlated with increasing CH_4:CO_2 ratio (Fig. 6a, $P < 0.001$), suggesting that acetate provided one of the important substrates for methanogenesis. The fact that acetate accumulated over time is due to the high SOC content (22.5 mmol total C g^{-1} dwt. soil) or high substrate availability in the organic layer. In the mineral layer, however, a reversed correlation was observed between acetate and CH_4:CO_2 ratio (Fig. 6b, $P < 0.02$), because methanogenesis was limited by the availability of acetate. Indeed, the CH_4:CO_2 ratio increased rapidly within the first 20-30 days (Fig. 2b), when acetate was being consumed (Fig. 4b), and the CH_4:CO_2 ratio leveled off after 30 days in the mineral layer. These observations are supported by our recent field measurements at BEO

388 showing an increased CH_4:CO_2 ratio but decreased acetate concentrations from early soil thaw in
389 July to deep thaw in late August (Herndon et al., 2015).

390 We also observed reduction of ferric ions in both organic and mineral layers, suggesting
391 that methanogenesis is not limited by the presence of Fe(III), consistent with previous studies in
392 Arctic soils (Lovley and Phillips, 1986; Reiche et al., 2008; Lipson et al., 2010; Siegert et al.,
393 2011; Roy Chowdhury et al., 2015), which differ from other studies where inhibited CH_4
394 production was observed with Fe(III) reduction (Metje and Frenzel, 2007; Lipson et al., 2012;
395 Miller et al., 2015). Dissolved Fe(III) or iron oxide minerals can serve as terminal electron
396 acceptors to facilitate the oxidation of SOC, and our results indicate that reducing sugars and
397 ethanol were continuously degraded to form more oxidized products (e.g., acetate, propionate,
398 butyrate, and ultimately CO_2) during early incubation, while the Fe(II)/Fe(total) ratios exhibited a
399 general increasing trend (Fig. 3, 4). In addition, glucose addition not only stimulated production
400 of organic acids but also increased Fe(II)/Fe(tot) ratios in the soil (Fig. 4), further demonstrating
401 that Fe(III)-reduction was associated with SOC oxidation. Correlations also exist between acetate
402 and Fe(II)/Fe(tot) in both soils layers. A positive correlation exists between Fe(II) production and
403 acetate production in the organic layer (Fig. 7a, $P < 0.01$), but a negative correlation in the
404 mineral layer (Fig. 7b, $P < 0.02$), indicating that Fe(III) reduction corresponded with the
405 consumption of acetate. However, positive correlations between CH_4:CO_2 and Fe(II)/Fe(tot)
406 were observed in both soil layers, confirming concurrent Fe(III) reduction and methanogenesis
407 occurring in the soil (Fig. 7c, d).

408 **5. Conclusions**

409 This work provides direct molecular evidence for SOC transformations as influenced by
410 temperature in Arctic soils. Labile SOC including free-reducing sugars, ethanol, and organic
411 acids are the most vulnerable SOC components to decompose under anaerobic conditions, similar

to those reported recently in aerobic incubations (Drake et al. 2015). These labile SOC followed a degradation pathway from sugars to alcohols and to acids, and consumption of acetate was positively correlated with methanogenesis and Fe(III) reduction under our experimental conditions. This experimentally based conceptual framework for the labile SOC transformations links carbon fermentation, iron reduction and methanogenesis in the active layer soil under warming. Recommendations for future research include understanding the roles of microbial community in SOC decomposition, particularly the transformation of high molecular weight SOC pools, and the effects of interactions among microbes, enzymes, and minerals on SOC degradation rates. By focusing on DOC and its chemical composition during anaerobic SOC degradation we find that the decomposability of SOC is a key factor controlling the transformation pathways and the rate of CH_4 and CO_2 emission in the permafrost-related soils, and therefore organic substrate composition should not be overlooked in predictive models for future climate change in Arctic.

Acknowledgements

The authors would like to thank Wei Fang, Taniya Roy Chowdhury, Hongmei Chen, Xiangping Yin, and Tonia Mehlhorn for technical assistance and chemical analysis. The Next Generation Ecosystem Experiments (NGEE-Arctic) project is supported by the Office of Biological and Environmental Research in the DOE Office of Science. Oak Ridge National Laboratory is managed by UT-Battelle LLC for US DOE under contract DE-AC05-00OR22725.

References:

Drake, T. W., Wickland, K. P., Spencer, R. G. M., McKnight, D. M., and Striegl, R. G.: Ancient low–molecular-weight organic acids in permafrost fuel rapid carbon dioxide production upon thaw, Proc. Natl. Acad. Sci. USA, DOI:10.1073/pnas.1511705112, 2015.

Duddleston, K.N., Kinney, M.A., Kiene, R.P., Hines, M.E., 2002. Anaerobic microbial biogeochemistry in a northern bog: Acetate as a dominant metabolic end product. Global Biogeochemical Cycles 16, 9.

Fierer, N., Craine, J.M., McLauchlan, K., Schimel, J.P., 2005. Litter quality and the temperature sensitivity of decomposition. Ecology 86, 320-326.

Graham, D.E., Wallenstein, M.D., Vishnivetskaya, T.A., Waldrop, M.P., Phelps, T.J., Pfiffner, S.M., Onstott, T.C., Whyte, L.G., Rivkina, E.M., Gilichinsky, D.A., Elias, D.A., Mackelprang, R., VerBerkmoes, N.C., Hettich, R.L., Wagner, D., Wullschleger, S.D., Jansson, J.K., 2012. Microbes in thawing permafrost: the unknown variable in the climate change equation. Isme Journal 6, 709-712.

Grogan, P., Jonasson, S., 2005. Temperature and substrate controls on intra-annual variation in ecosystem respiration in two subarctic vegetation types. Global Change Biology 11, 465-475.

Hernández, D., Hobbie, S., 2010. The effects of substrate composition, quantity, and diversity on microbial activity. Plant Soil 335, 397-411.

Herndon E., Yang Z., Barger J., Janot N., Regier T., Graham D., Wullschleger S., Gu B., Liang L., 2015. Geochemical drivers of organic matter decomposition in the active layer of Arctic tundra. *Biogeochemistry*, in press.

Hershey, A.E., Northington, R.M., Whalen, S.C., 2014. Substrate limitation of sediment methane flux, methane oxidation and use of stable isotopes for assessing methanogenesis pathways in a small arctic lake. Biogeochemistry 117, 325-336.

Hines, M.E., Duddleston, K.N., Kiene, R.P., 2001. Carbon flow to acetate and C-1 compounds in northern wetlands. Geophysical Research Letters 28, 4251-4254.

Hines, M.E., Duddleston, K.N., Rooney-Varga, J.N., Fields, D., Chanton, J.P., 2008. Uncoupling of acetate degradation from methane formation in Alaskan wetlands: Connections to vegetation distribution. Global Biogeochemical Cycles 22, 12.

Horn, M.A., Matthies, C., Kusel, K., Schramm, A., Drake, H.L., 2003. Hydrogenotrophic methanogenesis by moderately acid-tolerant methanogens of a methane-emitting acidic peat. Applied and Environmental Microbiology 69, 74-83.

Hugelius, G., Strauss, J., Zubrzycki, S., Harden, J.W., Schuur, E., Ping, C.-L., Schirrmeister, L., Grosse, G., Michaelson, G.J., Koven, C.D., 2014. Estimated stocks of circumpolar permafrost carbon with quantified uncertainty ranges and identified data gaps. Biogeosciences 11, 6573-6593.

Hung, C.C., Tang, D.G., Warnken, K.W., Santschi, P.H., 2001. Distributions of carbohydrates, including uronic acids, in estuarine waters of Galveston Bay. Marine Chemistry 73, 305-318.

Jagadamma, S., Mayes, M.A., Steinweg, J.M., Schaeffer, S.M., 2014. Substrate quality alters the microbial mineralization of added substrate and soil organic carbon. Biogeosciences 11, 4665-4678.

476 Kirchman, D.L., Hanson, T.E., Cottrell, M.T., Hamdan, L.J., 2014. Metagenomic analysis of
477 organic matter degradation in methane-rich Arctic Ocean sediments. Limnology and
478 Oceanography 59, 548-559.

479 Koven, C.D., Lawrence, D.M., Riley, W.J., 2015. Permafrost carbon-climate feedback is
480 sensitive to deep soil carbon decomposability but not deep soil nitrogen dynamics.
481 Proceedings of the National Academy of Sciences of the United States of America 112,
482 3752-3757.

483 Lee, H., Schuur, E.A.G., Inglett, K.S., Lavoie, M., Chanton, J.P., 2012. The rate of permafrost
484 carbon release under aerobic and anaerobic conditions and its potential effects on climate.
485 Global Change Biology 18, 515-527.

486 Lipson, D.A., Jha, M., Raab, T.K., Oechel, W.C., 2010. Reduction of iron (III) and humic
487 substances plays a major role in anaerobic respiration in an Arctic peat soil. Journal of
488 Geophysical Research-Biogeosciences 115, 13.

489 Lipson, D.A., Raab, T.K., Goria, D., Zlamal, J., 2013. The contribution of Fe(III) and humic
490 acid reduction to ecosystem respiration in drained thaw lake basins of the Arctic Coastal
491 Plain. Global Biogeochemical Cycles 27, 399-409.

492 Lipson, D.A., Zona, D., Raab, T.K., Bozzolo, F., Mauritz, M., Oechel, W.C., 2012. Water-table
493 height and microtopography control biogeochemical cycling in an Arctic coastal tundra
494 ecosystem. Biogeosciences 9, 577-591.

495 Lovley, D.R., Phillips, E.J.P., 1986. Organic-matter mineralization with reduction of ferric iron
496 in anaerobic sediments. Applied and Environmental Microbiology 51, 683-689.

497 McCalley, C.K., Woodcroft, B.J., Hodgkins, S.B., Wehr, R.A., Kim, E.H., Mondav, R., Crill,
498 P.M., Chanton, J.P., Rich, V.I., Tyson, G.W., Saleska, S.R., 2014. Methane dynamics
499 regulated by microbial community response to permafrost thaw. Nature 514, 478-+.

500 Metje, M., Frenzel, P., 2005. Effect of temperature on anaerobic ethanol oxidation and
501 methanogenesis in acidic peat from a northern wetland. Applied and Environmental
502 Microbiology 71, 8191-8200.

503 Metje, M., Frenzel, P., 2007. Methanogenesis and methanogenic pathways in a peat from
504 subarctic permafrost. Environmental Microbiology 9, 954-964.

505 Miller, K.E., Lai, C.T., Friedman, E.S., Angenent, L.T., Lipson, D.A., 2015. Methane
506 suppression by iron and humic acids in soils of the Arctic Coastal Plain. Soil Biology &
507 Biochemistry 83, 176-183.

508 Myklestad, S.M., Skanoy, E., Hestmann, S., 1997. A sensitive and rapid method for analysis of
509 dissolved mono- and polysaccharides in seawater. Marine Chemistry 56, 279-286.

510 Pare, M.C., Bedard-Haughn, A., 2013. Soil organic matter quality influences mineralization and
511 GHG emissions in cryosols: a field-based study of sub- to high Arctic. Global Change
512 Biology 19, 1126-1140.

513 R Core Team (2013): A Language and Environment for Statistical Computing. R Foundation
514 for Statistical Computing, Austria, Vienna. Available at: http://www.r-project.org.

515 Reiche, M., Torburg, G., Kusel, K., 2008. Competition of Fe(III) reduction and methanogenesis
516 in an acidic fen. Fems Microbiology Ecology 65, 88-101.

517 Riley, W.J., Subin, Z.M., Lawrence, D.M., Swenson, S.C., Torn, M.S., Meng, L., Mahowald,
518 N.M., Hess, P., 2011. Barriers to predicting changes in global terrestrial methane fluxes:

519 analyses using CLM4Me, a methane biogeochemistry model integrated in CESM.
520 Biogeosciences 8, 1925-1953.

521 Roy Chowdhury, T., Herndon, E.M., Phelps, T.J., Elias, D.A., Gu, B.H., Liang, L.Y.,
522 Wullschleger, S.D., Graham, D.E., 2015. Stoichiometry and temperature sensitivity of
523 methanogenesis and CO2 production from saturated polygonal tundra in Barrow, Alaska.
524 Global Change Biology 21, 722-737.

525 Schink, B., Phelps, T.J., Eichler, B., Zeikus, J.G., 1985. Comparison of ethanol degradation
526 pathways in anoxic fresh-water environments. Journal of General Microbiology 131, 651-
527 660.

528 Schulz, S., Conrad, R., 1996. Influence of temperature on pathways to methane production in
529 the permanently cold profundal sediment of Lake Constance. Fems Microbiology Ecology
530 20, 1-14.

531 Schuur, E.A.G., Bockheim, J., Canadell, J.G., Euskirchen, E., Field, C.B., Goryachkin, S.V.,
532 Hagemann, S., Kuhry, P., Lafleur, P.M., Lee, H., Mazhitova, G., Nelson, F.E., Rinke, A.,
533 Romanovsky, V.E., Shiklomanov, N., Tarnocai, C., Venevsky, S., Vogel, J.G., Zimov, S.A.,
534 2008. Vulnerability of permafrost carbon to climate change: Implications for the global
535 carbon cycle. Bioscience 58, 701-714.

536 Schuur, E. A. G., McGuire, A. D., Schadel, C., Grosse, G., Harden, J. W., Hayes, D. J.,
537 Hugelius, G., Koven, C. D., Kuhry, P., Lawrence, D. M., Natali, S. M., Olefeldt, D.,
538 Romanovsky, V. E., Schaefer, K., Turetsky, M. R., Treat, C. C., and Vonk, J. E., 2015.
539 Climate change and the permafrost carbon feedback, Nature, 520, 171-179.

540 Schuur, E.A.G., Vogel, J.G., Crummer, K.G., Lee, H., Sickman, J.O., Osterkamp, T.E., 2009.
541 The effect of permafrost thaw on old carbon release and net carbon exchange from tundra.
542 Nature 459, 556-559.

543 Siegert, M., Cichocka, D., Herrmann, S., Grundger, F., Feisthauer, S., Richnow, H.H.,
544 Springael, D., Kruger, M., 2011. Accelerated methanogenesis from aliphatic and aromatic
545 hydrocarbons under iron- and sulfate-reducing conditions. Fems Microbiology Letters 315,
546 6-16.

547 Tang, J.Y., Riley, W.J., 2015. Weaker soil carbon-climate feedbacks resulting from microbial
548 and abiotic interactions. Nature Climate Change 5, 56-60.

549 Tarnocai, C., Canadell, J.G., Schuur, E.A.G., Kuhry, P., Mazhitova, G., Zimov, S., 2009. Soil
550 organic carbon pools in the northern circumpolar permafrost region. Global Biogeochemical
551 Cycles 23, 11.

552 Tavendale, M.H., Meagher, L.P., Pacheco, D., Walker, N., Attwood, G.T., Sivakumaran, S.,
553 2005. Methane production from in vitro rumen incubations with Lotus pedunculatus and
554 Medicago sativa, and effects of extractable condensed tannin fractions on methanogenesis.
555 Animal Feed Science and Technology 123–124, Part 1, 403-419.

556 Treat, C.C., Natali, S.M., Ernakovich, J., Iversen, C.M., Lupascu, M., McGuire, A.D., Norby,
557 R.J., Roy Chowdhury, T., Richter, A., Šantrůčková, H., Schädel, C., Schuur, E.A.G., Sloan,
558 V.L., Turetsky, M.R., Waldrop, M.P., 2015. A pan-Arctic synthesis of CH4 and CO2
559 production from anoxic soil incubations. Global Change Biology 21, 2787-2803.

560 Tveit, A.T., Urich, T., Frenzel, P., Svenning, M.M., 2015. Metabolic and trophic interactions
561 modulate methane production by Arctic peat microbiota in response to warming.
562 Proceedings of the National Academy of Sciences of the United States of America 112,
563 E2507-E2516.

564 Waldrop, M.P., Wickland, K.P., White, R., Berhe, A.A., Harden, J.W., Romanovsky, V.E.,
565 2010. Molecular investigations into a globally important carbon pool: permafrost-protected
566 carbon in Alaskan soils. Global Change Biology 16, 2543-2554.

567 Wild, B., Schnecker, J., Alves, R.J.E., Barsukov, P., Bárta, J., Čapek, P., Gentsch, N., Gittel, A.,
568 Guggenberger, G., Lashchinskiy, N., Mikutta, R., Rusalimova, O., Šantrůčková, H.,
569 Shibistova, O., Urich, T., Watzka, M., Zrazhevskaya, G., Richter, A., 2014. Input of easily
570 available organic C and N stimulates microbial decomposition of soil organic matter in arctic
571 permafrost soil. Soil Biology and Biochemistry 75, 143-151.

572

Figure1

Fig. 1. Production rates of CH_4 (circle) and CO_2 (triangle) during anaerobic incubations of the organic (a, c) and mineral (b, d) layer soils from the Barrow Environmental Observatory (BEO), Barrow, Alaska, USA. Closed and open symbols represent data collected at temperatures of 8 and –2 ºC, respectively. Glucose and tannic acid were added to the soils at 8 ºC incubations only on day 144 and 188, respectively.

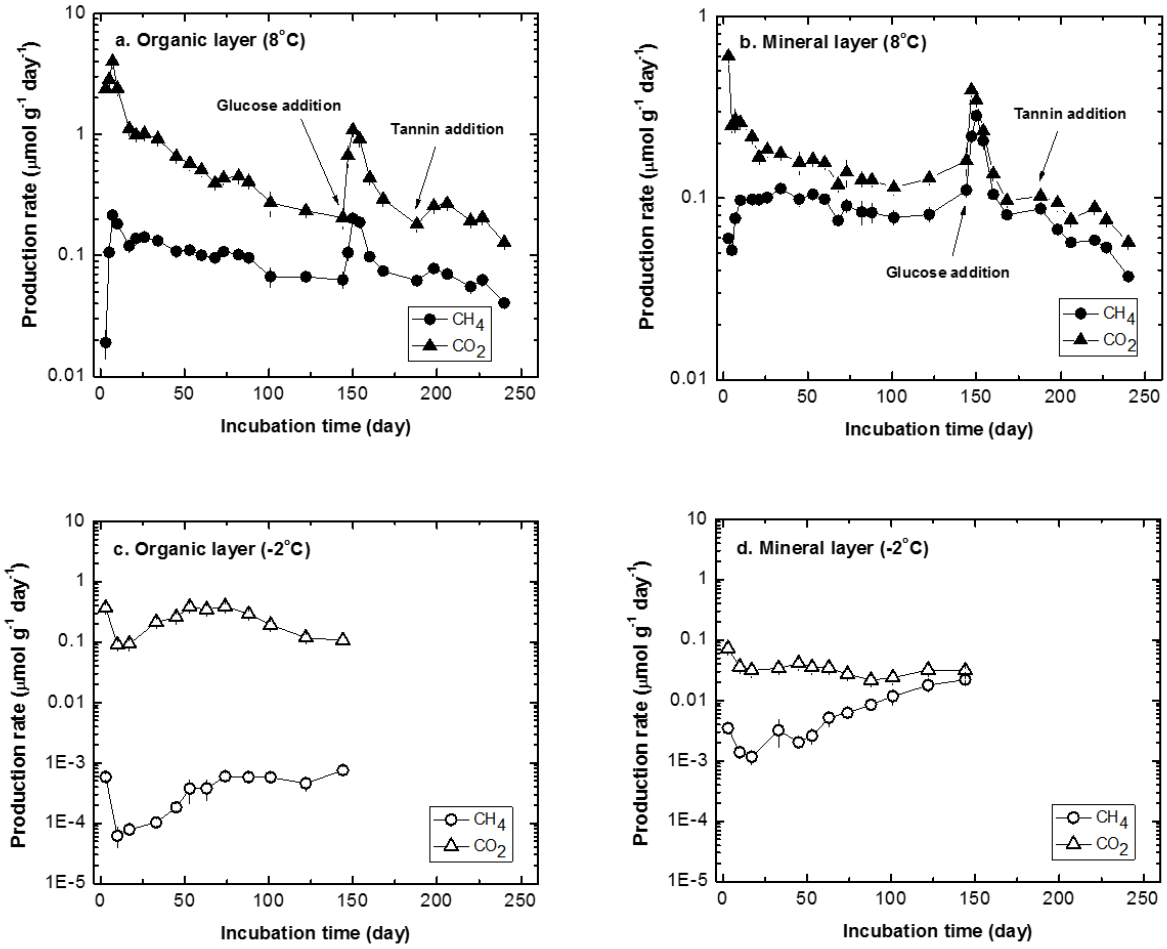

Figure2

Fig. 2. CH_4:CO_2 production ratios during anaerobic incubations of the organic layer and the mineral layer soils from BEO. Closed and open symbols represent data collected at temperatures at 8 and –2 ºC, respectively. Error bars represent one standard deviation of measurements from triplicate samples.

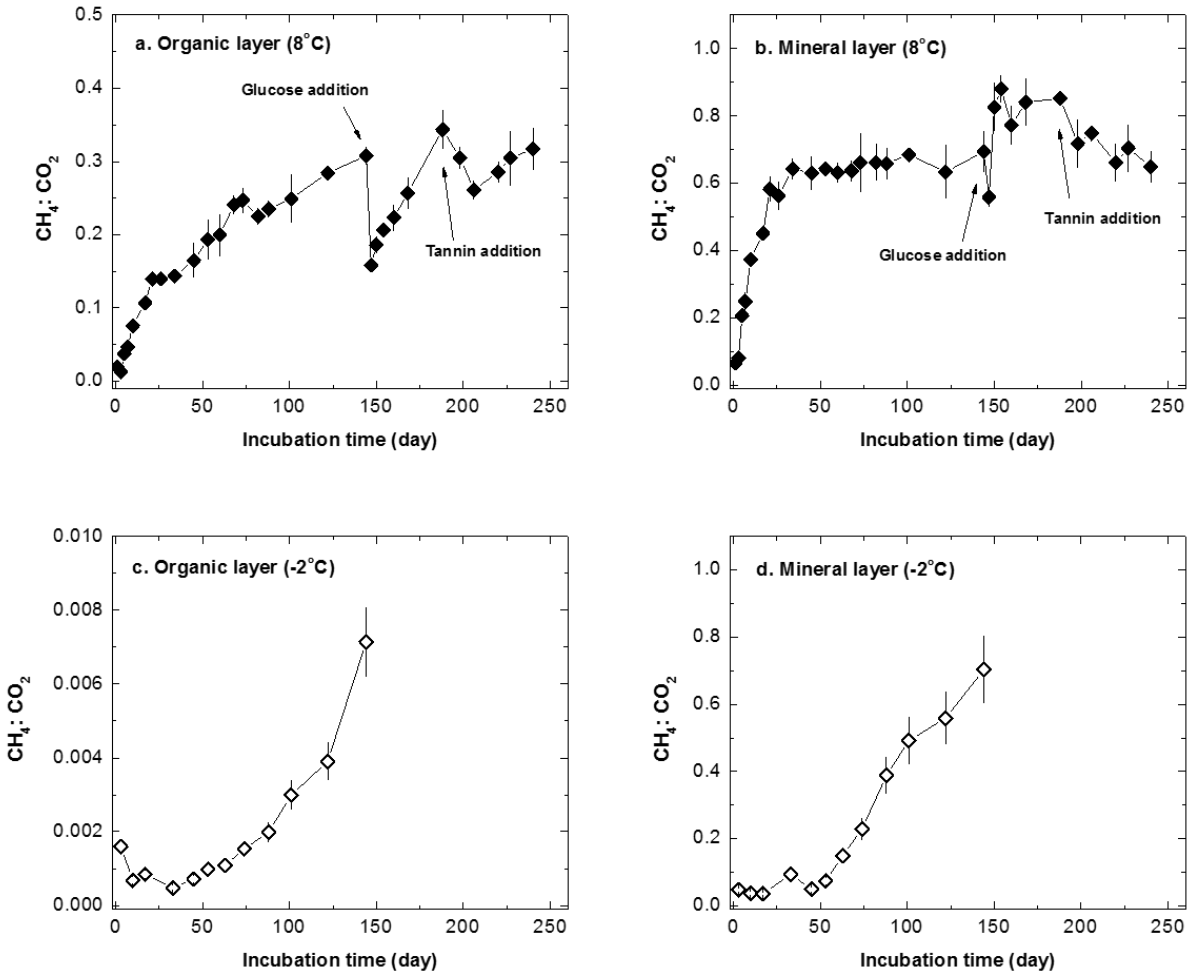

Figure3

Fig. 3. Concentration changes of free-reducing sugars (glucose equivalent) and ethanol during anaerobic incubations of the organic layer (a, c) and mineral layer soils (b, d). Closed and open symbols represent data collected at 8 and –2 ºC, respectively. Glucose and tannic acid were added to the 8 ºC microcosms on day 144 and 188, and error bars represent one standard deviation from triplicate sample measurements.

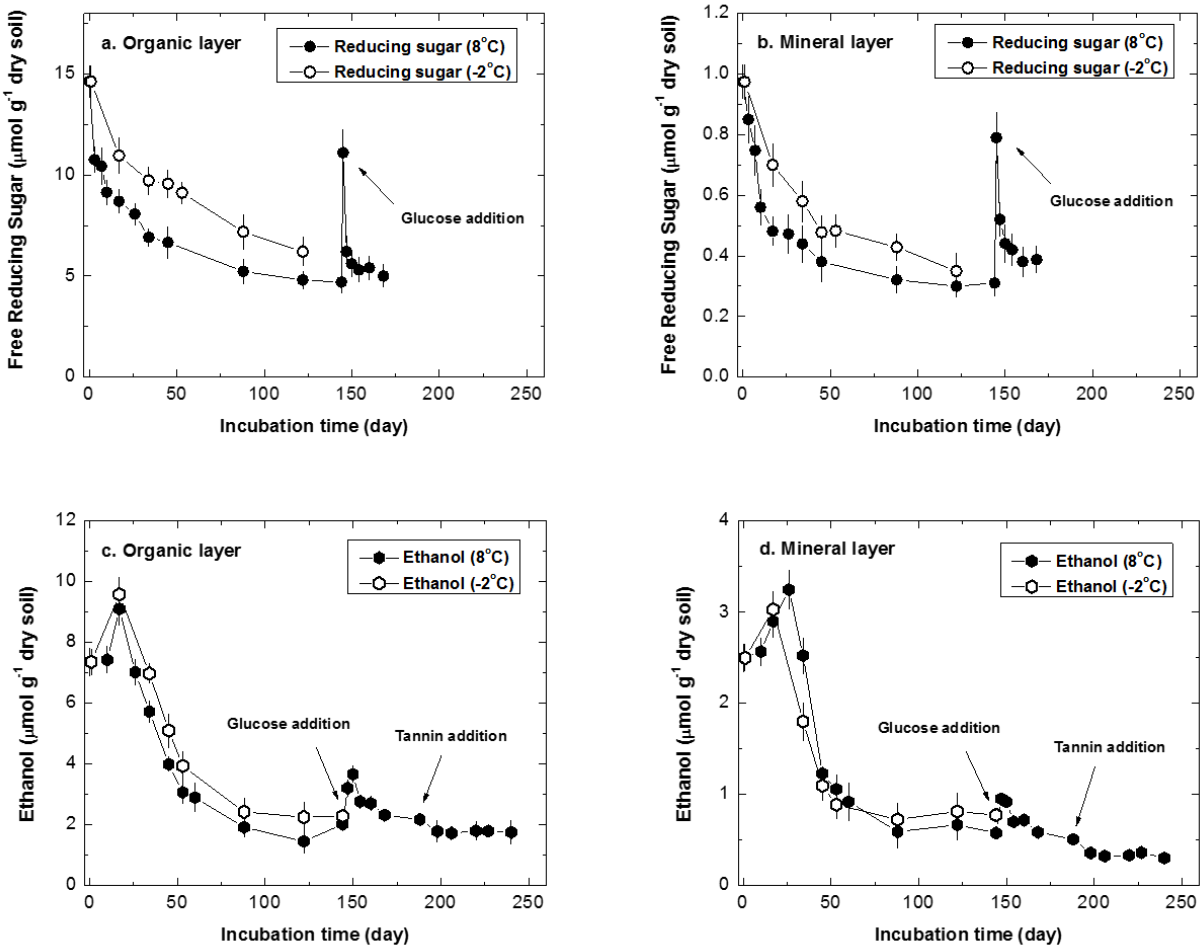

Figure4

Fig. 4. The production or consumption of formate (open circle), acetate (open triangle), propionate (open square), and butyrate (open diamond) during anaerobic incubations of the organic (a, c) and mineral (b, d) layer soils at 8 and –2 ºC, respectively. Glucose and tannic acid were added to the 8 ºC microcosms on day 144 and 188, and error bars represent one standard deviation from triplicate sample measurements.

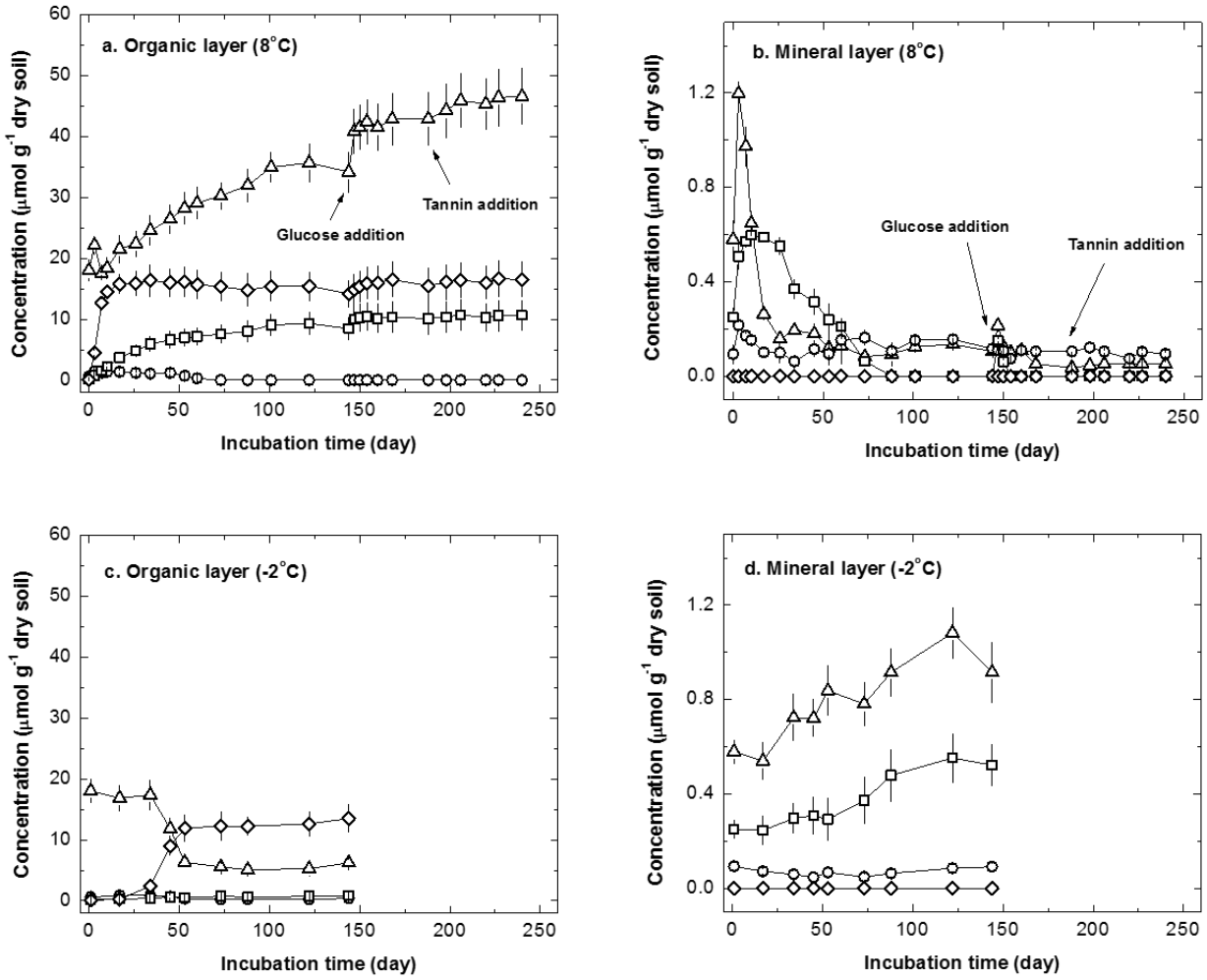

Figure5

Fig. 5. Conceptual model of anaerobic soil organic carbon (SOC) degradation pathways and the production or consumption of labile organic carbon substrates in the active layer upon warming. Numbers in parentheses refer to the proposed pathways of SOC degradation (see text for additional details).

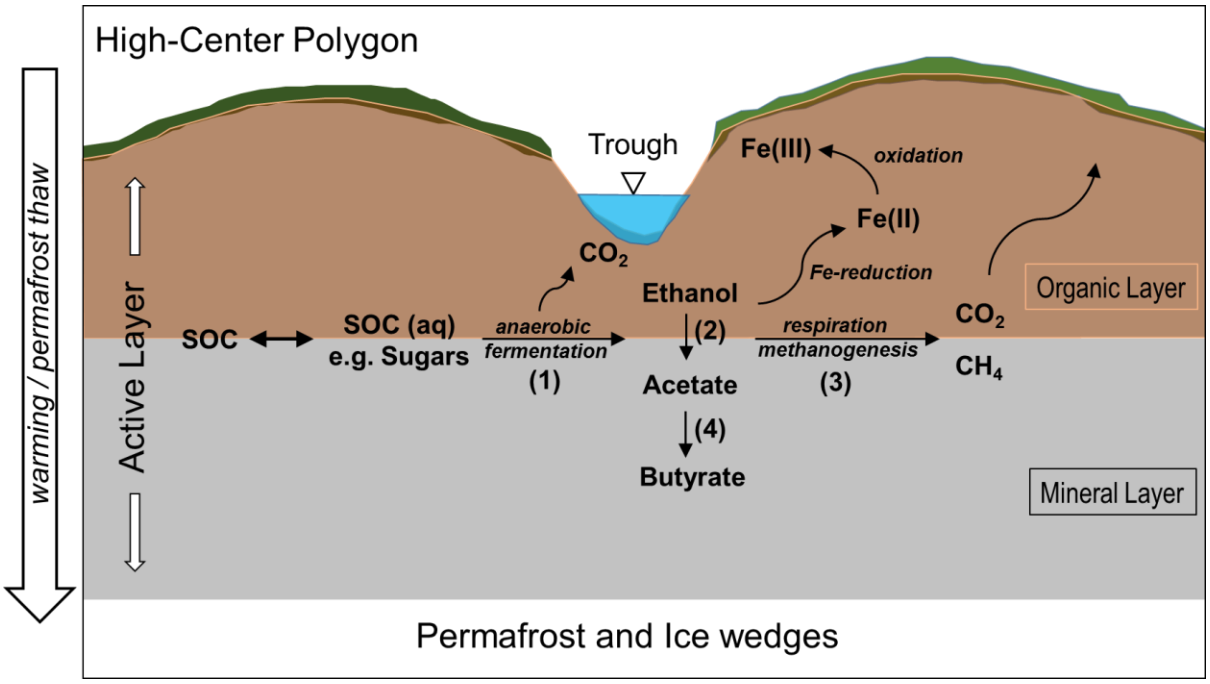

Figure6

Fig. 6. Correlations between acetate production and CH_4:CO_2 production ratios during anaerobic incubations of the organic (a) and mineral (b) layer soils at 8 ºC. Open circles and triangles represent the data points collected respectively before and after glucose addition on day 144, and solid lines indicate the best fits of the data.

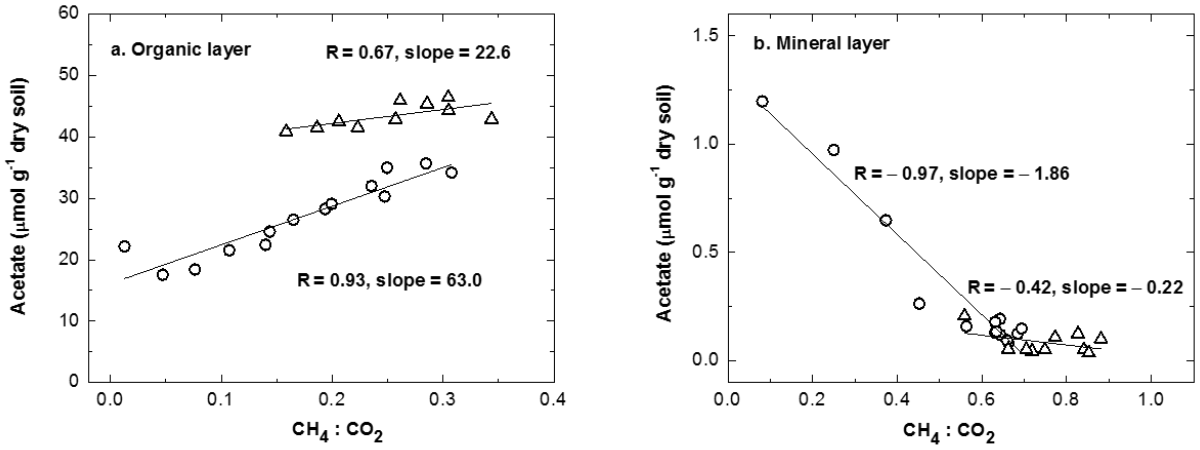

Figure7
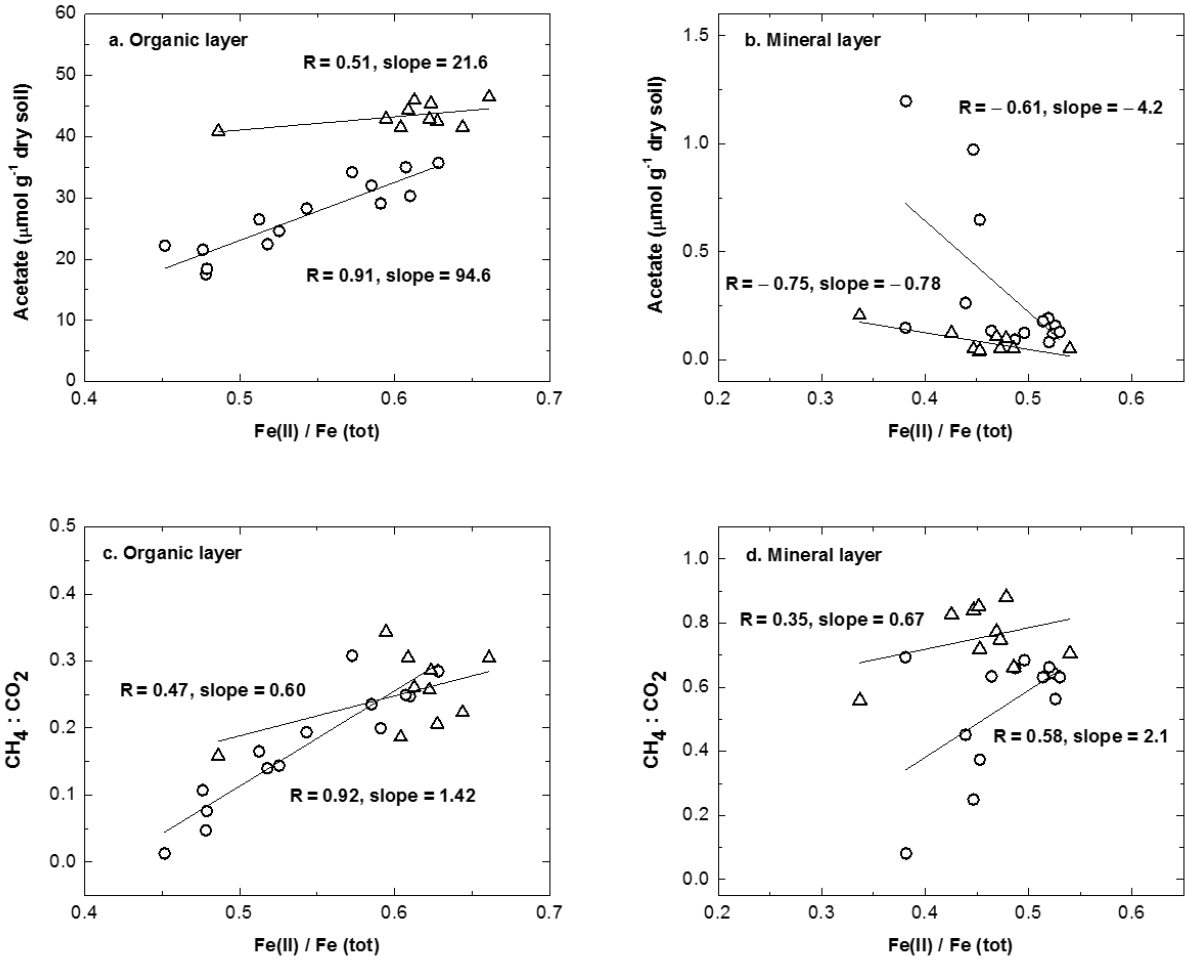
Fig. 7. Correlations between acetate production and Fe(II)/Fe(tot) ratios in the organic (a) and mineral (b) layer soils, and between CH_4:CO_2 and Fe(II)/Fe(tot) in the organic (c) and mineral (d) layer soils. All data were collected from the anaerobic incubations at 8 ºC. Open circles and triangles represent the data collected before and after the glucose addition on day 144, respectively. Solid lines indicate the best fits.